JOURNAL OF MATERIALS SCIENCE **36** (2001) 1343–1347

# In-depth deformation of InP under a Vickers indentor

G. PATRIARCHE
*France Telecom, Centre National d'Etudes des Télécommunications, Laboratoire Concepts des Dispositifs pour la Photonique, BP. 107, F 92225 Bagneux Cedex, France*
*E-mail: gilles.patriarche@rd.francetelecom.fr*

E. LE BOURHIS
*Université de Poitiers, Laboratoire de Métallurgie Physique, UMR 6630 CNRS, SP2MI-Téléport 2-Bd Marie et Pierre Curie, BP 30179, F 86962 Futuroscope-chasseneuil Cedex, France*

(001) surfaces of InP single crystals have been deformed at room temperature by a Vickers indentor submitted to a load of 1 N. The indents formed were observed by transmission electron microscopy (TEM) in cross-sectional views obtained by the focused-ion beam (FIB) technique. The structure of the plastic zone has been investigated and the different modes of plastic deformation involved during the deformation have been analysed. The flow stress of InP was estimated and compared to the reported values in the literature.


## 1. Introduction

In the field of semiconductor studies, the indentation test has been used to elucidate the relationship between mechanical and electrical properties. This test has been applied to generate dislocations of a known type ($\alpha$ or $\beta$) in order to study their electrical activity [1–3] or to determine the relative mobility of $\alpha$ or $\beta$ dislocations [4]. The case of a (001) face of GaAs has been extensively investigated [5–7]. It was shown that the activated slip planes were those on which the calculated elastic stress generated by the indentor was maximum. A V structure of the rosette arm was proposed in good agreement with the two-fold symmetry of the rosette [4]. The deepest part of the plastic zone in indented (001) InP was only investigated by cathodoluminescence (CL) in a scanning electron microscope [8]. In this work, the plastic deformation into the sample could be described very well by four slip flows along the ⟨011⟩ directions inclined to the surface. Here we have used the focused-ion beam (FIB) technique and transmission electron microscopy (TEM) to investigate the structure of the plastic zone as well as the dislocation arrangement generated at room temperature by a Vickers indentor in indium phosphide.

## 2. Experimental techniques

The Czochralski-grown single crystals of iron-doped indium phosphide ($10^{18}$ at·cm$^{-3}$) were oriented along a ⟨001⟩ direction. The samples were deformed at room temperature in air by a Testwell indentor using a Vickers diamond pyramid. The applied force was about 1 N and the indentor was left 30 s on the sample before being raised up. The loading and unloading rates were about 1 mm/min.

To prepare the TEM cross-sectional thin foils, the FIB technique was used. The specimens were milled using a 30 kV Gallium-ion beam. The zone selected for TEM observations was protected from the Gallium ions by a Tungsten thin film. Two trenches were milled in such a way that a thin wall was left containing the selected zone transparent to the electron beam (Fig. 1). It must be noted that when a crack was present, the Tungsten film was inefficient to protect the surface from ion-milling.

The crystal polarity was determined by convergent-beam electron diffraction as proposed by Tafto and Spence [9]. CBED patterns obtained on a {110} cross-sectional thin foil are shown in Fig. 2a. The Bragg conditions were fulfilled for the [1, 1, 9] and [1, 1, 11] reflections. In these conditions, two black crossing lines were observed in the [002] spot as the two reflections mentioned before interfere destructively with the [002] reflection. Therefore, the thin foil wall could be determined as a ($1\bar{1}0$) plane (Fig. 1). The zincblende structure in the [110] projection is shown in Fig. 2b. Following Warren *et al*. [4], $\alpha$ dislocations are expected to extend along the [110] direction while $\beta$ dislocations are expected along the [110] direction.

## 3. Results and discussion

### 3.1. Plastic zone structure

A cross-sectional view made in the centre of the indentation is shown in Fig. 3. The indentation profile is observed in the right part of the figure and only one half of the plastic zone is shown. The inclination of the indent face to the surface of the sample is about 16°. This is 5° less than the inclination between a Vickers diamond face and the surface of the sample (22°). This

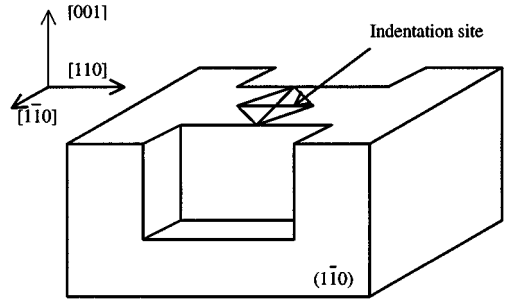


*Figure 1* Geometry of the TEM specimens prepared for cross-sectional views.

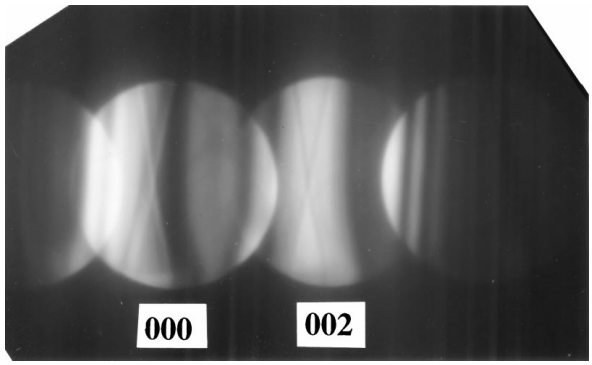


(a)

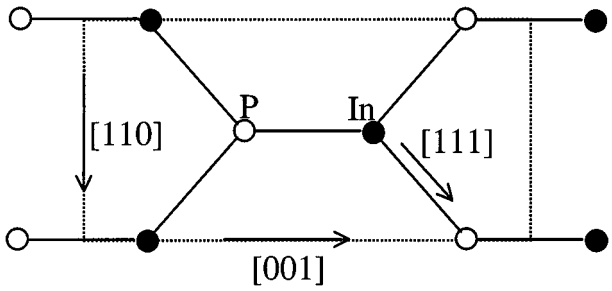


(b)

*Figure 2* (a) CBED patterns. Bragg conditions were fulfilled for the [002], [1, 1,9] and [1, 1, 11] reflections. In the [002] spot, black crossing lines can be observed. (b) The zincblende structure in the [1$\bar{1}$0] projection. The dark full circles represent P atoms and the dark empty circles represent In atoms.

difference is attributed to the elastic recovery during load removal [10].

Just beneath the indentation site, it was very difficult to image the sample, as the material was highly disturbed. The diffraction patterns taken in this zone showed elongated spots attributed to the local misorientations of the crystal generated by the large deformations. The disorientation was estimated to be about 10 °.

Underneath this very perturbed zone, that is at 5 $\mu$m in-depth and below, the diffraction spots recovered a circular shape. From this depth and down to about 20 $\mu$m, plastic deformation was observed. In the deepest part, the lateral extension of the plastic zone was about 40 $\mu$m for an indenting load of 1 N.

The plastic deformation was highly heterogeneous as very dense slip bands were observed in cross-section (Fig. 3). They correspond to concentrated plastic deformation in adjacent slip planes. At the bottom and in the lateral parts of the plastic zone, individual dislocations could be observed. At the surface of the sample, individual dislocation lines extended to about 20 $\mu$m away from the indent site.

Thereafter, the structure of the plastic zone is schematised in Fig. 4. The rosette arms correspond to the most superficial plastic zone that is generally observed at the surface of III-V semiconductors deformed by indentation [4].

The deepest part of the plastic zone with a roof-shape structure is drawn. Its width increases with depth.

The inclination of the dense slip bands to the surface was about 54°. They are contained in {111} planes. Such slip bands either converged underneath the indentation site or diverged from it.

The roof-shape zone has a square base whose sides are parallel to the ⟨110⟩ directions contained in the (001) plane. The {111} sides of the pyramid intersect along the four ⟨011⟩ directions inclined to the surface. This structure is very consistent with the CL observations of sulphur-doped indium phosphide indented at 400°C [8].

### 3.2. Plastic deformation modes

Diffraction patterns of a zone containing several slip bands are shown in Fig. 5a. Additional spots due to microtwinning can be observed. The slip bands responsible for the twinning spots of Fig. 5a could be identified using the additional spot to form the image of the zone (Fig. 5b).

Furthermore, using the $g = [004]$ diffraction condition, most of the dislocations did not vanish (Fig. 6). Therefore, the Burgers vectors of the dislocations constituting such slip bands are inclined to the surface. Such dislocations participate to the vertical material flow.

Inclined $b = a/2\langle 011\rangle$ Burgers vectors of perfect dislocations are of four types and parallel to the intersections of the {111} roof shape zone sides. It must be noted that partial dislocations have Burgers vectors of type $b = a/6\langle 112\rangle$ which are necessarily inclined to the surface.

The few perfect dislocations vanishing using the $g = [004]$ diffraction condition, are arrowed in Fig. 6. Using the vanishing condition ($g \cdot b = 0$), the Burgers vector of these dislocations is parallel to the surface. Using the $g = [220]$ diffraction condition, such dislocations didn't vanish so that we conclude that $b = a/2[110]$. Therefore, the long segments observed in Fig. 6 aligned along the [110] direction are of screw character. Similar dislocation lines have already been observed in plan view by TEM at the surface of indented samples [11]. The material flow generated by such dislocations is lateral. However, in view of the low number of them, the induced material flow is much reduced compared to the vertical flow generated by the dislocations with Burgers vector inclined to the sample surface.

### 3.3. Critical stress and flow stress of InP at room temperature

In the deepest part of the plastic zone, parallel perfect 60° dislocations lines could be observed separated by about 60 nm (Fig. 7). This distance corresponds to a

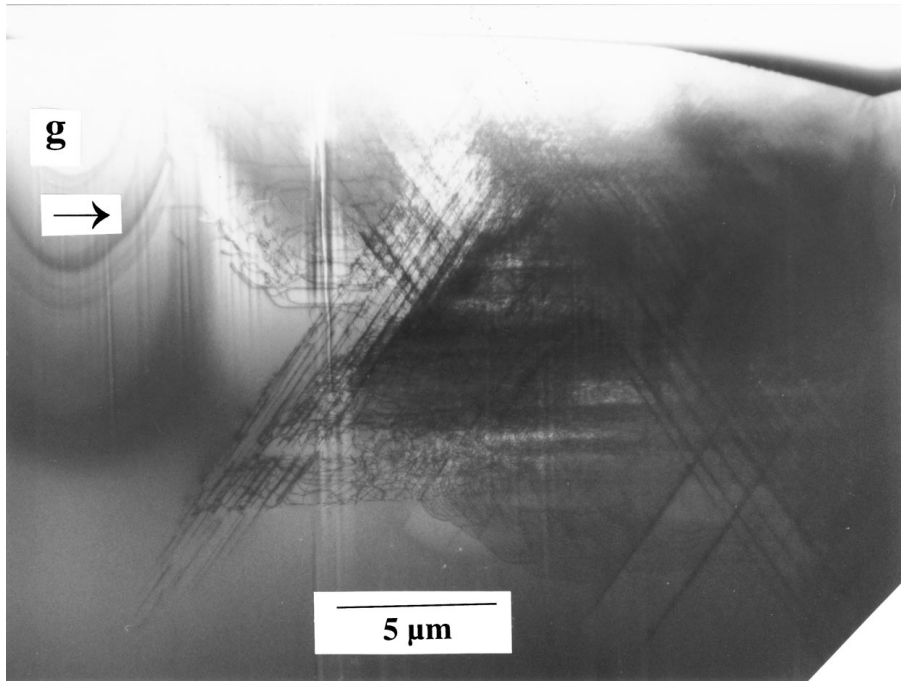


*Figure 3* TEM cross-sectional view of InP sample indented at room temperature under 1 N. The indent profile can be observed on the right side of the micrograph. Only one half of the plastic zone is shown.

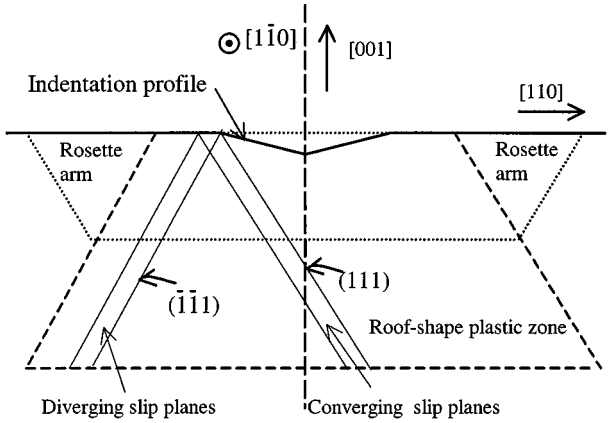


*Figure 4* Schematic representation of the plastic zone structure. The rosette arm as well as the roof-shape zone are drawn with dotted lines. The projection of the converging and diverging slip planes in the ($1\bar{1}0$) plane are drawn with continuous lines.

distance between dislocations of about 75 nm in their {111} slip plane.

The leading dislocation is submitted to repulsive elastic forces from the other dislocations and to the image force of the free surface that we have neglected here in view of the depth of the plastic zone (Fig. 8).

The equilibrium of the leading dislocation (Burgers vector $b$) is reached when the elastic forces $F_k$ due to the other dislocations (numbered $k$) are balanced by the critical stress $\tau$ necessary to move a dislocation:

$$\tau b = \sum_{k=1}^{n} F_k = \sum_{k=1}^{n} \frac{A}{r_k}$$

with $r_k$ the distance between the leading dislocation and the other dislocations. As a first approximation, we considered only the ten nearest dislocations and we

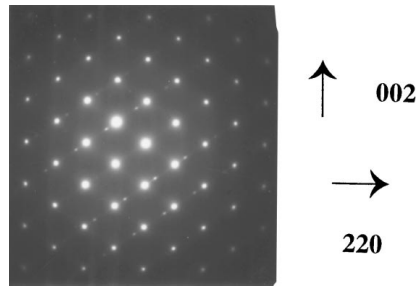


(a)

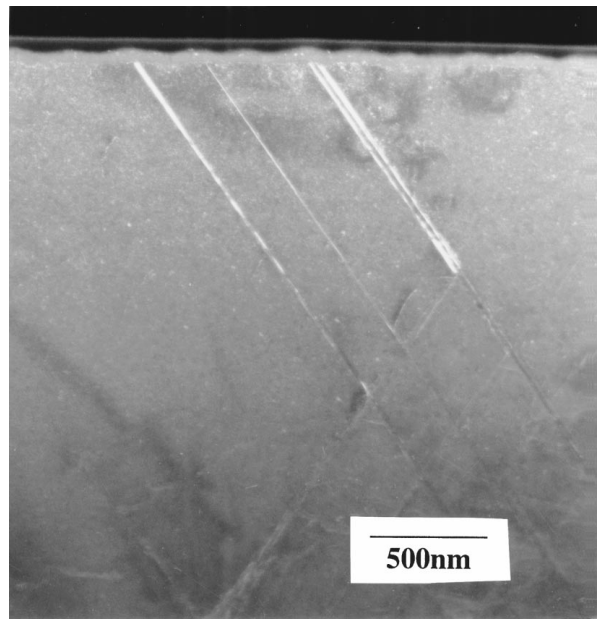


(b)

*Figure 5* (a) Diffraction patterns taken in the left-side region of Fig. 3. Spots associated with microtwinning can be observed. (b) TEM cross-sectional view using an additional diffraction spot associated with microtwinning. The indentation is situated on the right side of the micrograph. The internal planes containing microtwinning are in contrast on the figure.

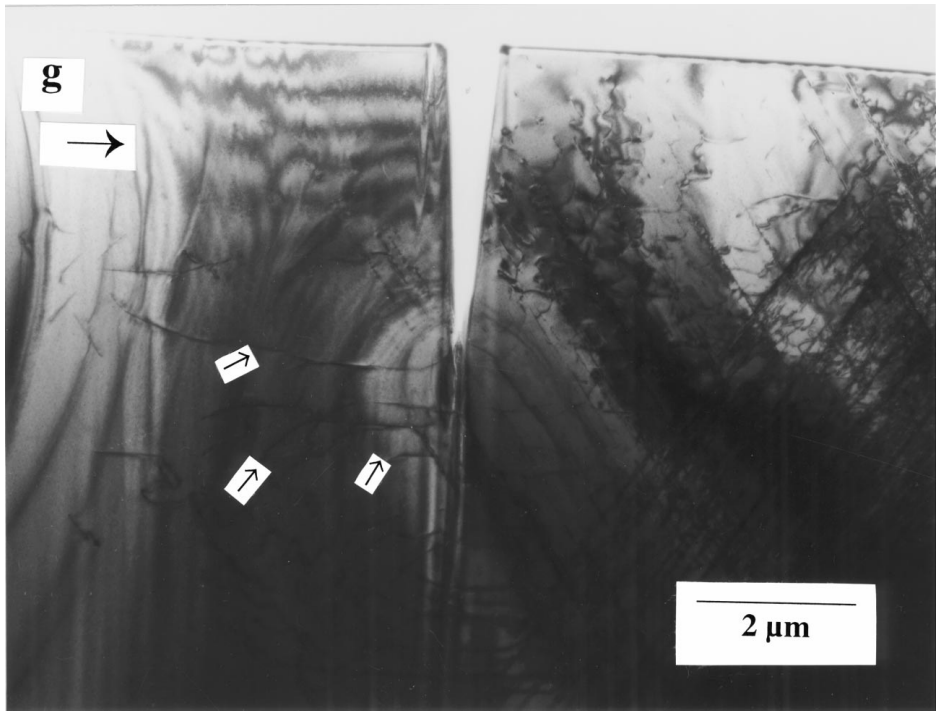


(a)

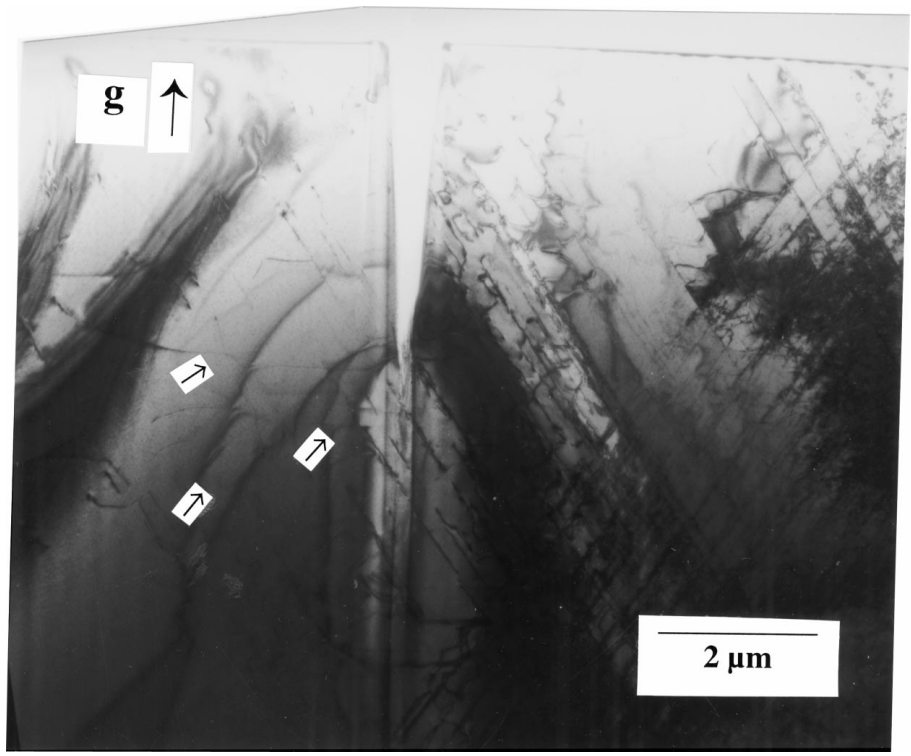


(b)

*Figure 6* Higher-magnification image of the left-side region of Fig. 3 (rosette arm in Fig. 4). (a) $g = [220]$ diffraction condition, (b) $g = [004]$ diffraction condition. Only a few dislocations vanished using the $g = [004]$ diffraction condition (see arrows). The vertical trench is the result of the ion-milling of a zone that contained a crack.

assumed that all of them had the same Burgers vector $b$ and were of edge character so that $A$ can be written [12]:

$$A = \frac{\mu b^2}{2\pi(1-\nu)}$$

where $\mu$ is the shear modulus, $\nu$ the Poisson's ratio. Using $\mu = 39$ GPa, $\nu = 0.3$ and $b = 0.4$ nm, we estimated the critical stress necessary to move a perfect dislocation to be about 150 MPa.

On the other hand, using the Johnson's relation between the plastic zone radius $c$ and the square root of the load $F$, we could determine the flow stress $Y$ of InP at room temperature [13]:

$$c = \sqrt{\frac{3F}{2\pi Y}}$$

Taking for $c$ the value of the plastic zone depth (20 $\mu$m), the flow stress was estimated to be about

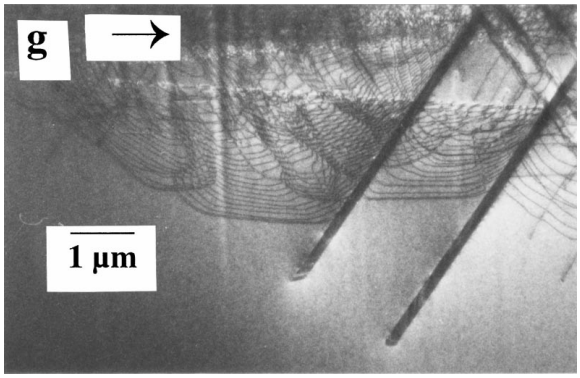


*Figure 7* Higher-magnification image of the bottom of the roof-shape zone (arrowed in Fig. 3) showing parallel dislocation lines ($g = [220]$ diffraction condition).

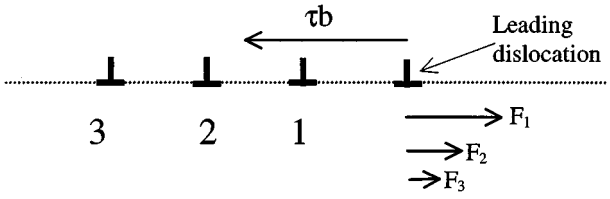


*Figure 8* Schematic representation showing a leading dislocation (Burgers vector $b$) and the repulsive elastic forces $F_k$ from the other dislocations. $\tau$ is the critical stress necessary to move the leading dislocation.

700 MPa. Using the diagonal length of the indentation measured on images obtained in the FIB scanning microscope (about 25 $\mu$m), the Vickers hardness $H_v$ was determined to be about 2.9 GPa. This yields a $H_v/Y$ ratio of about 4 when it is expected to be about 3 [13]. This discrepancy is attributed to the crack generation and development. Such cracks can be avoided using low loads (nanoindentation techniques). In a former paper, we reported measurements on various III-V semiconductors with loads ranged between 600 $\mu$N and 10000 $\mu$N. We determined in all cases $H_v/Y$ ratio to be about 2.5 [14].

The determination of the critical stress necessary to move a dislocation underestimates the value as we considered only the ten nearest dislocations. Nonetheless, this value is much less than the flow stress determined using the relation of Johnson [13]. In fact, interactions between dislocations are very likely in the dense region situated just beneath the indentation site. These interactions may even lead to work hardening forming Lomer-Cottrell locks [6]. The determination using the relation of Johnson takes work hardening into account. In comparison, dislocations at the bottom of the plastic zone encounter only few native dislocations. Interactions between dislocations are to be considered in the relevant part of the stress-strain curve that is used to determine the critical resolved shear stress. Suzuki *et al*. [15] reported for InP a resolved shear stress of about 350 MPa at room temperature that is intermediate between the critical stress and the flow stress values determined here.

## 4. Conclusion

The deformation of iron-doped InP at room temperature under a Vickers indentor is highly heterogeneous. Just beneath the indentor, the deformation is so great that crystal misorientations were observed. Concentrated deformation was observed in {111} slip bands. Mainly microtwinning and perfect dislocations with inclined Burgers vector were observed. Both deformation modes participate in the vertical material flow that is generated by the indentor. However, a few dislocations with Burgers vector parallel to the surface were observed.

The critical stress necessary to move a dislocation as well as the flow stress could be determined using two approaches. Firstly the positions of the dislocations at the bottom of the plastic zone were used to calculate the elastic forces on a leading dislocation. The equilibrium let us determine the critical stress necessary to move this dislocation. Secondly, assuming the relation of Johnson [13], the flow stress was determined using the size of the plastic zone. The critical stress was estimated to be about 150 MPa and found to be about four times less than the flow stress (700 MPa). This is attributed to work hardening beneath the indentor. In fact, dislocation interactions are likely in this region and may even lead to Lomer-Cottrell locks [6].

## Acknowledgements

The authors are very grateful to J. P. Rivière for fruitful discussions and to D. Chassaing for technical assistance.

## References

1. A. ZOZIME, I. HANKE and W. SCHRÖTER, *Phys. Stat. Sol.* (a) **138a** (1993) 445.
2. T. WOZINSKI, A. ZOZIME, A. RIVIÈRE and C. VERMELIN, *ibid.* **142a** (1994) 673.
3. B. SIEBER, J. L. FARVACQUE and A. MIRI, *ibid.* **138a** (1993) 673.
4. P. D. WARREN, P. PIROUZ and S. G. ROBERTS, *Phil. Mag.* **A50** (1984) L23.
5. P. B. HIRSCH, P. PIROUZ, S. G. ROBERTS and P. D. WARREN, *ibid.* **B52** (1985) 759.
6. S. G. ROBERTS, P. D. WARREN and P. B. HIRSCH, *J. Mater. Res.* **1** (1986) 162.
7. *Idem., Mater. Sci. Engng.* **A105/106** (1988) 19.
8. E. LE BOURHIS, J. P. RIVIERE and A. ZOZIME, *J. Mater. Sci.* **31** (1996) 6571.
9. J. TAFTO and J. C. H. SPENCE, *J. Appl. Cryst.* **15** (1982) 60.
10. W. C. OLIVER and G. M. PHARR, *J. Mater. Res.* **7** (1992) 1564.
11. C. LEVADE and G. VANDERSCHAEVE, *Phys. Stat. Sol.* (a) **171a** (1999) 83.
12. J. P. HIRTH and J. LOTHE, in "Theory of Dislocations" (Wiley Interscience, 1982).
13. K. L. JOHNSON, in "Contact Mechanics" (Cambridge University Press, 1985).
14. G. PATRIARCHE and E. LE BOURHIS, *J. Mater. Sci. Lett.*, in press.
15. T. SUZUKI, T. YASUTOMI and T. TOKUAKA, *Phil. Mag.* **A79** (1999) 2637.

*Received 28 March*
*and accepted 19 October 2000*